Available online at www.sciencedirect.com

SCIENCE DIRECT®

Polymer 46 (2005) 12366–12371

polymer

www.elsevier.com/locate/polymer

New kinetic aspects on the mechanism of thermal oxidative degradation of polypropylenes with various tacticities

Hisayuki Nakatani [a,*], Shoutarou Suzuki [b], Takamasa Tanaka [b], Minoru Terano [b]

[a] *Department of Bioengineering and Chemistry, College of Environment Engineering and Architecture, Kanazawa Institute of Technology, 7-1 Ohgiga-oka, Nonoichi, Ishikawa 921-8501, Japan*

[b] *School of Material Science, Japan Advanced Institute of Science and Technology, 1-1 Asahidai, Tatsunokuchi, Ishikawa 923-1292, Japan*

Received 28 July 2005; received in revised form 21 October 2005; accepted 28 October 2005

Available online 14 November 2005

Abstract

Thermal oxidative degradation behavior of polypropylene (PP) with different tacticities was studied based on the activation energy (ΔE) data obtained by thermogravimetric analysis (TGA). The ΔE value showed a negative proportion to the content of meso pentad fraction (*mmmm*) in all of isotactic PP (iPP) samples, and that of syndiotactic PP sample considerably deviated from this negative proportion relationship. Since the value of *mmmm* was directly related to polymer chain conformation, the ΔE value was thought to have close connection with the concentration of 3_1 helix conformation in the iPPs. The ΔE changes would be caused by the competition between uni- and bimolecular hydroperoxide decomposition, which was controlled by concentration and character of conformations of PPs.

© 2006 Elsevier Ltd. All rights reserved.

Keywords: Polypropylene; Thermal oxidative degradation; Tacticity

1. Introduction

There is much literature on mechanisms of oxidative degradation of polypropylene (PP) [1–6]. Many researchers agree fundamentally with the following mechanistic scheme:

Initiation:

$$\mathrm{RH} \rightarrow \mathrm{R}\cdot \tag{I}$$

Propagation:

$$\mathrm{R}\cdot + \mathrm{O_2} \rightarrow \mathrm{ROO}\cdot \tag{II}$$

$$\mathrm{ROO}\cdot + \mathrm{RH} \rightarrow \mathrm{R}\cdot + \mathrm{ROOH} \tag{III}$$

Chain branching (including chain scission):

$$\mathrm{ROOH} \rightarrow \text{carbonyls} + \mathrm{R}\cdot \tag{IV}$$

$$\mathrm{ROOH} + \mathrm{ROOH} \rightarrow \text{carbonyls} + \mathrm{R}\cdot \tag{V}$$

Detailed study on the early stage of thermal oxidative degradation called 'induction period' was performed by many researchers. According to Audouin et al. [4], the calculated activation energy (ΔE) of unimolecular hydroperoxide decomposition accompanied with molecular weight loss, corresponding to (IV), was about $100\ \mathrm{kJ\,mol^{-1}}$, and the half value (ca. $50\ \mathrm{kJ\,mol^{-1}}$) was estimated for the bimolecular hydroperoxide decomposition (V). Moreover, in coexistence of unimolecular and bimolecular hydroperoxides, using model compounds, the values of $137\ \mathrm{kJ\,mol^{-1}}$ and $119\ \mathrm{kJ\,mol^{-1}}$ were estimated for the decompositions of unimolecular and bimolecular hydroperoxide, respectively [6]. Owing to being influenced by various factors such as kind of PP sample and measurement condition, it is difficult to compare each of ΔE values directly. It seems, however, that the ΔE value of bimolecular hydroperoxide decomposition is lower than that of unimolecular one at least.

With regard to hydroperoxide production, the study on the formation reaction originated from alkane model has been carried out in many years. Krorcek et al. estimated that the ΔE in the formation reaction of hydroperoxide from tertiary peroxy radical (corresponding to (III)) was about $62\ \mathrm{kJ\,mol^{-1}}$ using an empirical equation [7]. Whereas, Audouin et al. reported that the ΔE of hydroperoxide production of isotactic PP (iPP), corresponding to (II) and (III), was $90\ \mathrm{kJ\,mol^{-1}}$ in a relatively low temperature range (50–70 °C) [8].

Such kinetic study on the degradation of iPP has been performed actively since the calculated kinetic parameters,

---

* Corresponding author. Tel.: +81 76 248 9970; fax: +81 76 294 6713.
E-mail address: h-nakatani@neptune.kanazawa-it.ac.jp (H. Nakatani).

0032-3861/$ - see front matter © 2006 Elsevier Ltd. All rights reserved.
doi:10.1016/j.polymer.2005.10.131

such as ΔE, have contributed to the clarification of the complicated mechanism of degradation.

In our previous work [9], the dependence of tacticity in thermal oxidative degradation was investigated using PPs with various tacticities. The results suggested that the degradation stability become higher with the decrease in meso pentad fraction (*mmmm*). However, this dependence was qualitatively derived from thermogravimetric analysis (TGA) in air. Relationship between the disorder of tacticity and the stability has not been quantitatively clear yet. As described above, the acquisition of quantitative parameter, such as the activation energy, is useful for the clarification of degradation mechanism. When each of the degradation activation energy of the PPs is calculated, a relationship between the *mmmm* and the rate of degradation appears to be clear. Simultaneously the influence of superstructure on the rate of degradation can be estimated since the value of *mmmm* has a close relation to the formation of specific super structure such as helical conformation. Calculation of degradation activation energy will provide an opportunity to clarify characteristics of oxidative degradation of PP.

In this study, with aim of clarifying the characteristics of oxidative degradation of PP, values of degradation activation energy in PPs with various tacticities were calculated by TGA, and the relationship between the degree of tacticity and the change of activation energy was studied in detail.

2. Experimental

2.1. Materials

Propylene of research grade (donated by Chisso Corp.), anhydrous $MgCl_2$ and $TiCl_3$ (donated by Toho Titanium Co., Ltd), nitrogen (purchased from Uno Sanso Co.), and triethylaluminum (TEA) (donated by Tosoh Finechem Co.) were used without further purification. TEA was used as a toluene solution. Toluene was purified by passing through a molecular sieves 13Xcolumn.

2.2. Catalyst preparation

In order to obtain PP with different tacticity distribution, a $TiCl_3$-based Ziegler catalyst was used. The catalyst was prepared by grinding $MgCl_2$ and $TiCl_3$ by a 1.2 L stainless steel vibration mill pot with 55 balls (25 mm diameter) under nitrogen atmosphere for 30 h at room temperature. The Ti content of catalyst was 0.05 mmol-Ti/g-cat. The catalyst was used as toluene slurry.

2.3. Polymerization

The PP having broad tacticity distribution was synthesized using the grinded $TiCl_3/MgCl_2$ and triethylaluminium (TEA) catalyst system. Polymerization was performed at Al/Ti molar ratio of ca. 2 at 30 °C for 30 min in toluene as a solvent. In order to remove catalyst residues, The PP was reprecipitated from a boiling xylene solution into methanol under nitrogen atmosphere.

2.4. Higher isotactic and syndiotactic polypropylenes

Isotactic and syndiotactic PPs were supplied by Toho Catalyst Co, Ltd and Mitsui Chemicals Inc., respectively. In order to remove unfavorable catalyst residues and stabilizers, these PPs were stirred with distilled water containing a small amount of ethanol at room temperature overnight, dried, and then were reprecipitated from a boiling xylene solution into methanol under nitrogen atmosphere.

2.5. Thermal oxidative degradation in the solid

Thermal oxidative degradation was performed at 130 °C for 10–120 min in air. The heater (Senshu SSC-9300) was used for examination. No additional antioxidant was used in all cases. Sample was dried in vacuo at 60 °C for 3 h. Then 5 mg of each powdery sample in a small vial was allowed to stand in a heater. In the heater, the vial was covered with a heating jacket to achieve effective heat transfer to the sample.

2.6. GPC characterization of PP

After the thermal oxidative degradation, the degraded PP in the small vial was dissolved in 5 ml of *o*-dichlorobenzene containing 2,6-di-*t*-butyl-*p*-cresol as an antioxidant, and the obtained PP solution was directly measured by GPC. In the meantime, degraded PP solution was sucked up to the small vial and dried with N_2 flow. Then it was dissolved in 5 ml of *o*-dichlorobenzene (ODCB) containing antioxidant. The molecular weight of PP sample was determined by GPC (Senshu, SSC-7100) with styrene-divinylbenzene gel columns (SHODEX, HT-806M) at 140 °C using *o*-dichlorobenzene as a solvent.

2.7. ^{13}C NMR measurement of PP

Primary structure was determined by ^{13}C NMR measurement using a Varian Gemini-300 spectrometer at 120 °C on 20% (w/v) solution in hexachloro-1,3-butadiene. 1,1,2,2-tetrachloroethane-d2 was added as an internal lock and used as an internal chemical shift reference.

2.8. TREF analysis of PPs

The tacticity distribution of PP was determined by temperature rising elution fractionation (TREF: Senshu, SSC-7300) with ODCB as an extraction solvent, which contains same antioxidant. A fraction column packed with Chromosorb (bought from Celite Corp.) with 10 mm diameter and 30 cm in length was used for the TREF characterization. About 70 mg of each PP sample was dissolved in 10 ml of ODCB at 140 °C, and a part of the solution (ca. 6 ml) was passed through the fraction column, which was slowly cooled down at 6.7 °C h^{-1} from 140 to 20 °C simultaneously. Elution of the deposited PP with ODCB at a flow rate of 150 ml h^{-1} was first carried out at 20 °C for 30 min to obtain the ODCB-soluble fraction, and then the column was heated at 16 °C h^{-1} up to 140 °C. The eluted PP solution was analyzed by a refractive index detector to obtain the TREF diagram. Moreover, tacticity fractions of the polymer with increasing crystallinity were then eluted with ODCB at temperatures increasing stepwise. Extraction took place over temperatures ranging from 20 to 140 °C divided into 5 steps (20, 60, 90, 106 and 140 °C). Polymer was eluted during 90 min at every step after the temperature had stabilized for 30 min. Tacticity fractions were then collected and precipitated in methanol. All of fractionated PPs were the TREF diagrams of insoluble parts above 20 °C. The weight fraction of soluble part (below 20 °C) was 52 wt%, and its molecular weight ($M_n = 6000$) and tacticity (*mmmm* = 25) were very low, respectively. Since this soluble part was considered to contain little impurities such as unsaturated polymer chain end groups for promoting degradation [10], it was completely removed.

2.9. Thermal analysis of PP

Melting temperature (T_m) of PP was determined by a differential scanning calorimeter (DSC, METTER DSC 820). Without the preheating, the DSC measurement was performed from 20 to 200 °C at a heating rate of 10 °C min^{-1} under nitrogen atmosphere (nitrogen flow rate: 200 ml min^{-1}). The decrease in weight of PP was analyzed by a thermogravimetric analysis (TGA, METTER TG50) at 130 °C for 40 h under air (air flow rate: 50 ml min^{-1}).

3. Results and discussion

Isotactic PP (original iPP) having a broad tacticity distribution was synthesized by a $TiCl_3$ based Ziegler catalyst system as reported in the previous paper [9]. Each of iPPs with various tacticities was obtained from fractionation of the original iPP using TREF. The fraction ratio and the molecular weight are summarized in Table 1. The nomenclature used in this paper is as follows: e.g. iPP76 denotes iPP with the *mmmm* of around 76 mol%. All pentad fractions of the iPPs are shown in Table 2.

Table 1
Fraction ratio and molecular weight of fractionated iPPs

Sample	Range of elution temperature	Fraction ration (wt%)	$\bar{M}_n$ [a] (g mol^{-1})	$\bar{M}_w/\bar{M}_n$
–	20	52	0.6×10^4	–
iPP52	20–60	17	1.1×10^4	4.6
iPP76	60–90	12	1.8×10^4	5.1
iPP87	90–106	9	2.5×10^4	3.2
iPP91	106–140	10	7.4×10^4	8.5

[a] Measured by GPC.

The weight change curves of TGA are shown in Fig. 1. Thermal oxidative degradation is performed at the constant temperature (130 °C) in air atmosphere. The weight changes of iPPs display multi-stages with advance of degradation [11,12]. A period of constant weight, namely induction period, is initially seen, and then the weight is increasing by oxidation. Beyond maximum, weight loss increases with volatilized component, and finally mass balance becomes negative. Here, the increase of the weight, which means the end of an induction period, has started earlier as the *mmmm* becomes higher. The results indicate that the initiation reaction of degradation depends strongly on the isotacticity.

In order to evaluate this dependence quantitatively, in all iPPs, the durations of induction period (t_{di}) have been determined using the weight change curves obtained from the measurements at several constant temperatures (130, 135, 140 and 145 °C). As shown in Fig. 2, t_{di} has been defined as the time (second) at the intersection of the tangent at the inflection point with the plateau line of induction period. The values of t_{di} are summarized in Table 3. These values have been processed into Arrhenius plots. As shown in Fig. 3, the t_{di} obeys the Arrhenius law apparently within the chosen temperature limit. Table 4 gives values of the apparent activation energy (ΔE).

Here is one question as to the kind of reaction to correspond to the ΔE. It is known that the oxidative degradation of PP proceeds through autoxidation reaction. In the early stage, this autoxidation is cycle reaction ('closed loop') [4,6,11,12], which consists of the production reactions of peroxy radical ((II); see Section 1), of hydroperoxide ((III); see Section 1), and the decomposition reactions of unimolecular ((IV); see Section 1) and bimolecular ((V); see Section 1) hydroperoxides. In fact, the occurrence of (II) and (III) has been determined since the increasing of weight was observed at t_{di} (see Fig. 2). As with the production reactions, the reaction of the hydroperoxide decompositions accompanied with the decrease in molecular weight has simultaneously occurred during the induction period. For instance, as shown in Fig. 4, the changes in ratio of molecular weight ($M_{n,t}/M_{n,0}$) of iPPs can be seen considerably early as compared with the time of t_{di} in Table 3. The obtained ΔE should correspond to the rate-determining step of reaction in this autoxidation. Among (II)–(V) reactions, since the production reaction of peroxy radical reaction (II) is a simple radical reaction with rapid rate and that

Table 2
^{13}C NMR pentad distribution (mol%) for iPPS

Sample	*mmmm*	*mmmr*	*rmmr*	*mmrr*	*mmrm* + *rrmr*	*mrmr*	*rrr*	*mrrr*	*mrrm*
iPP52	51.5	13.3	1.7	12.2	5.6	1.4	5.2	4.1	5.0
iPP76	76.3	9.8	0.0	7.0	2.0	0.0	1.8	0.6	2.5
iPP87	87.0	6.2	0.7	3.2	0.7	0.1	0.6	0.4	1.1
iPP91	90.6	6.5	0.4	1.4	0.3	0.1	0.1	0.1	0.5

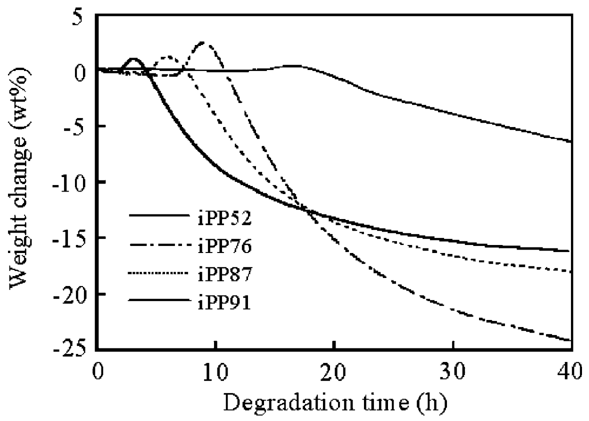

Fig. 1. Weight change curves of iPPs at 130 °C.

of (III) is a considerably lower ΔE [7], (II) and (III) are believed to be not the rate-determining step. The hydroperoxide decompositions (IV) and (V) will be the rate-determining step. As shown in Section 1, considering the data of some reports[4,6,7], it seems that the ΔE of unimolecular hydroperoxide decomposition is higher than that of the hydroperoxide production, suggesting that the decomposition is the rate-determining step. However, as shown in Table 4, the ΔE increases with the decrease in *mmmm* and this relationship is hardly explained when only the unimolecular hydroperoxide decomposition (IV) considers as the rate-determining step. If the formation rate of bimolecular hydroperoxide increases with the increase of tacticity, the observed ΔE changes can be explained by the competition between the unimolecular decomposition with a higher ΔE and bimolecular one with a lower ΔE [4,6].

In order to obtain more detailed information about the relationship between the tacticity and the ΔE, using higher isotactic PP (iPP95; $\bar{M}_n = 1.8 \times 10^4$ g mol^{-1}, $\bar{M}_w/\bar{M}_n = 4.9$) and syndiotactic PP (sPP; $\bar{M}_n = 5.7 \times 10^4$ g mol^{-1}, $\bar{M}_w/\bar{M}_n = 3.8$), their ΔE's were calculated as well as those of other iPPs. It can be considered that sPP is a specific iPP having '*mmmm* = 0'. Indeed, it has been reported that sPP exhibited resistance higher than iPP against thermal oxidative degradation [13–16]. All pentad fractions of the iPP95 and sPP are summarized in Table 5, and those values of t_{di} obey the Arrhenius law apparently within the chosen temperature limit (Fig. 5).

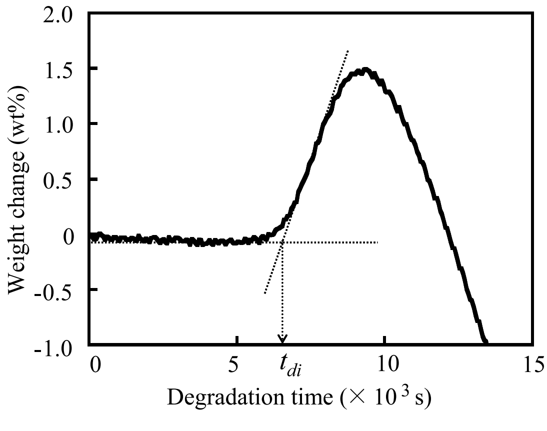

Fig. 2. An example of weight change curve showing a determination of the durations of induction period (t_{di}).

Table 3
Value of t_{di} of iPP at various temperature

Heating temp. (°C)	t_{di} ($\times 10^{-3}$ s)			
	iPP52	iPP76	iPP87	iPP91
130	49.0	31.2	15.8	8.7
135	18.1	17.1	9.6	6.6
140	16.0	13.1	6.3	4.3
145	6.8–7.6[a]	6.4	4.0	2.4

[a] The t_{di} of iPP52 scattered in this temperature considerably.

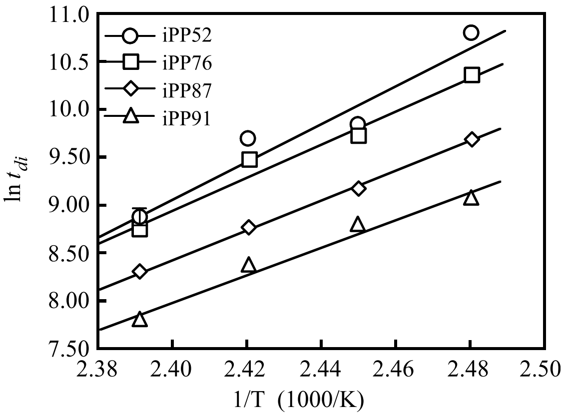

Fig. 3. Arrhenius plots of t_{di} for thermal oxidative degradation of iPPs.

Table 4
Apparent activation energy (ΔE)

Sample	ΔE (kJ mol^{-1})
iPP52	155.5–170.1[a]
iPP76	140.9
iPP87	127.8
iPP91	118.8

[a] Due to the scattering of t_{di} at 145 °C.

Audouin et al. proposed from a theoretical formula that the thermogravimetric (weight change) curve of mainly containing

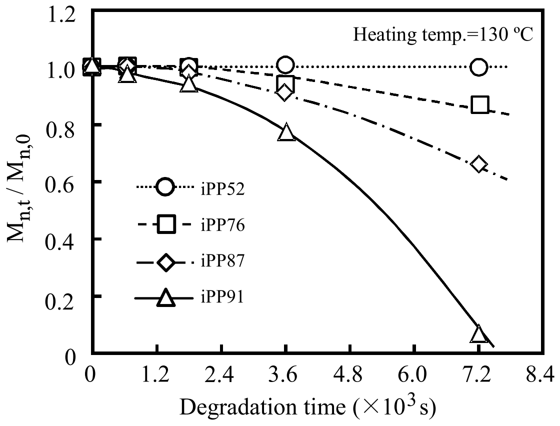

Fig. 4. Changes in ratio of molecular weight ($M_{n,t}/M_{n,0}$) of iPPs during thermal degradation: $M_{n,t}$ = number average molecular weight in a degradation time (t), $M_{n,0}$ = original number average molecular weight.

Table 5
^{13}C NMR pentad distribution (mol%) for iPP95 and sPP

Samples	*mmmm*	*mmmr*	*rmmr*	*mmrr*	*mmrm*+ *rrmr*	*mrmr*	*rrr*	*mrr*	*mrrm*
iPP95	94.5	4.1	0.0	0.8	0.4	0.0	0.0	0.0	0.2
sPP	0.0	0.3	2.3	4.2	3.0	0.7	79.2	10.3	0.0

bimolecular hydroperoxide becomes broader, and that the curve of mainly containing unimolecular one does sharper [11]. Interestingly, as shown in Fig. 6, the weight change curve of sPP is broad and of iPP95 is sharp, suggesting that the results are consistent with their ones and the ΔE is dependent on the kind of produced hydroperoxide.

All the data of ΔE are plotted against their *mmmm* as shown in Fig. 7. Of particular interest here is the dependence of ΔE on the content of *mmmm*. The ΔE is in negative proportion to the content of *mmmm* in all of iPPs. The relationship obeys the following equation:

$$\Delta E(\mathrm{kJ\ mol^{-1}}) = -1.24 \times [mmmm] + 205 \sim 235$$

This tendency will be related to the production rate of bimolecular hydroperoxide (Fig. 8) [17]. Here, the most interesting point is that the ΔE value of sPP considerably deviates from this equation (Fig. 7). We have already reported that the rate of degradation systematically depended on the tacticity and simply speculated that the closer tertiary hydrogen location, namely existence on the same side of hydrogen and peroxide radical, provided meso sequence with the driving force for acceleration of the hydroperoxide production [9]. However, the sPP deviation implies that the difference of primary structure such as tacticity is unable to sufficiently demonstrate this dependence.

The value of *mmmm* is directly related to superstructure such as polymer chain conformation. In the case of iPP, the chain conformation mainly takes a compact 3_1 helix conformation (TGTG) with the increase of *mmmm* [18]. Whereas, that of sPP takes a comparatively loose 4_1 helix conformation or a planar-zigzag conformation [18]. When the degradation reaction occurs in the 3_1 helix conformation, the distance between peroxy radical and tertiary C–H becomes closer due to not only the meso arrangement but the compact 3_1 helix conformation as well. Thus, the production of bimolecular hydroperoxide [17] advances more easily (Fig. 8). Presumably the peroxy radical and the tertiary C–H are spatially separated in the disordered 3_1 helix conformation, the 4_1 helix conformation and/or the planar-zigzag conformation, and their abstraction reactions are relatively hard to occur. The ΔE value seems to reflect only the concentration of 3_1 helix conformation in the iPPs. The observed ΔE changes is believed to be caused by the competition between uni- and bimolecular

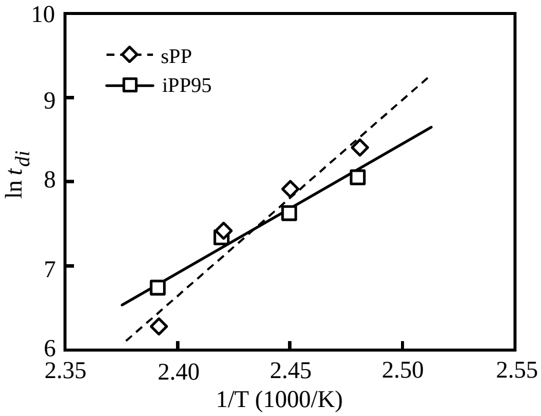

Fig. 5. Arrhenius plots of t_{di} for thermal oxidative degradation of iPP95 and sPP.

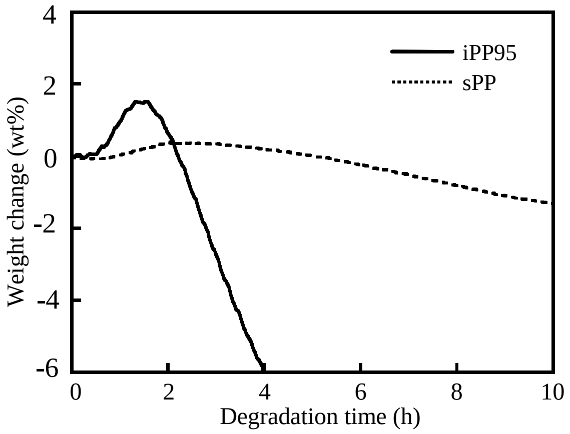

Fig. 6. Weight change curves of iPP95 and sPP at 135 °C.

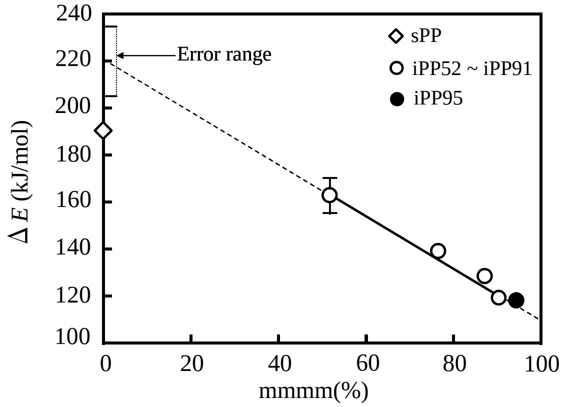

Fig. 7. Activation energy (ΔE) versus meso pentad fraction (*mmmm*) for all of degraded PPs.

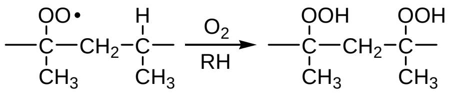

$$-\overset{\mathrm{OO\bullet}}{\underset{\mathrm{CH_3}}{\mathrm{C}}}-\mathrm{CH_2}-\overset{\mathrm{H}}{\underset{\mathrm{CH_3}}{\mathrm{C}}}- \xrightarrow[\mathrm{RH}]{\mathrm{O_2}} -\overset{\mathrm{OOH}}{\underset{\mathrm{CH_3}}{\mathrm{C}}}-\mathrm{CH_2}-\overset{\mathrm{OOH}}{\underset{\mathrm{CH_3}}{\mathrm{C}}}-$$

Fig. 8. Formation of bimolecular hydroperoxide by an intramolecular propagation reaction [17].

hydroperoxide decomposition and to be controlled by concentration and character of conformations of PPs.

In addition, all of the thermal oxidations have been performed over 130 °C. At such higher temperature [6,19], oxygen can be diffused sufficiently in the crystalline part, which consists of the 3_1 helix conformation. Under the condition of the negligible oxygen diffusion difference between crystalline and amorphous parts, the oxidative degradation will easily take place within the 3_1 helix conformation.

4. Conclusion

Dependence of tacticity in PP oxidative degradation was studied by the calculation of ΔE. The ΔE value was in negative proportion to the content of *mmmm* in all of iPPs. Whereas, the ΔE value of sPP (*mmmm* = 0) considerably deviated from this relationship. These results implied that only the difference in primary structure was unable to sufficiently clarify the characteristics of oxidative degradation. The value of *mmmm* was directly related to polymer chain conformation, and the ΔE value seemed to reflect the concentration of 3_1 helix conformation in the iPPs. The ΔE changes would be caused by the competition between uni- and bimolecular hydroperoxide decomposition, which was controlled by concentration and character of conformations of PPs.

Acknowledgements

This work was supported by the Grant-in-Aid for Scientific Research, No. 17550194 from Japan Society for the Promotion of Science.

References

[1] Kato Y, Carlsson DJ, Wiles DM. J Appl Polym Sci 1969;13:1447–58.
[2] Carlsson DJ, Wiles DM. Macromolecules 1969;6(2):597–606.
[3] Billingham NC. Makromol Chem Macromol Symp 1989;28:145–63.
[4] Audouin L, Gueguen V, Tcharkhtchi A, Verdu J. J Polym Sci, Part A: Polym Chem 1995;33:921–7.
[5] Alam MS, Nakatani H, Ichiki T, Goss Ben GS, Liu B, Terano M. J Appl Polym Sci 2002;86(8):1863–7.
[6] Achimsky L, Audouin L, Verdu J, Rychly J, Matisova-Rychla L. Polym Degrad Stab 1997;58:283–9.
[7] Korcek S, Chenier JHB, Howard JA, Ingold KU. Can J Chem 1972;50: 2285–97.
[8] Audouin L, Girois S, Achimsky L, Verdu J. Polym Degrad Stab 1998;60: 137–43.
[9] Suzuki S, Liu B, Terano M, Manabe N, Kawamura K, Ishikawa M, et al. Polym Bull 2005;54:311–9.
[10] Gómez-Elvira JM, Tiemblo P, Elvira M, Matisova-Rychla L, Rychly J. Polym Degrad Stab 2004;85:873–82.
[11] Audouin L, Achimsky L, Verdu J. In: Halim Hamid S, editor. Handbook of polymer degradation. 2nd ed. New York: Marcel Dekker; 2000. p. 727–63.
[12] Rychly J, Matisova-Rychla L, Csmorova K, Achimsky L, Audouin L, Tcharkhtchi A, Verdu J. Polym Degrad Stab 1997;58:269–74.
[13] Hatanaka T, Mori H, Terano M. Macromol Rapid Commun 1997;18: 157–61.
[14] Osawa Z, Kato M, Terano M. Macromol Rapid Commun 1997;18: 667–71.
[15] Hatanaka T, Mori H, Terano M. Polym Degrad Stab 1999;64:313–9.
[16] Kato M, Osawa Z. Polym Degrad Stab 1999;65:457–61.
[17] Zahradníčková A, Sedlář J, Dastych D. Polym Degrad Stab 1991;32: 155–76.
[18] He P, Xiao Y, Zhang P, Xing C, Zhu N, Zhu X, et al. Polym Degrad Stab 2005;88:473–9.
[19] Tiemblo P, Gómez-Elvira JM, Garcia Beltrán S, Matisova-Rychla L, Rychly J. Macromolecules 2002;35:5922–6.